Optica Applicata, Vol. XXXV, No. 3, 2005

Thermoreflectance and micro-Raman measurements of the temperature distributions in broad contact laser diodes

TOMASZ J. OCHALSKI[1], TOMASZ PIWOŃSKI[1], DOROTA WAWER[1], KAMIL PIERŚCIŃSKI[1], MACIEJ BUGAJSKI[1], ANNA KOZŁOWSKA[2], ANDRZEJ MALĄG[2], JENS W. TOMM[3]

[1]Institute of Electron Technology, al. Lotnikow 32/46, 02-668 Warszawa, Poland

[2]Institute of Electronic Materials Technology, ul. Wólczyńska 133, 01-919 Warszawa, Poland

[3]Max Born Institute for Nonlinear Optics and Short Pulse Spectrocopy, Max-Born 2A, D 12489 Berlin, Germany

In this paper we describe a number of optical techniques suitable for estimation of the semiconductor surface temperature. High spatially resolved thermoreflectance will be shown as a powerful tool to measure temperature distribution at the laser diode front facet. For determination of the absolute value of the front facet temperature we use micro-Raman spectroscopy. Both techniques will be presented as a complementary ways to determine surface temperature distribution on the working laser diode.

Keywords: thermoreflectance, Raman spectroscopy, semiconductor laser.

1. Introduction

The performance of a diode laser is strictly related to the temperature distribution in the laser structure and thus depends on the laser design, materials used for its construction and operating conditions. In this work we study temperature distributions at the mirrors in high power broad area laser diodes (LD). It should be noted that the temperature at the facet plays a critical role in device reliability and performance.

We will present 2D maps of relative temperature T distribution for p-side down mounted GaAsP/AlGaAs quantum well lasers with different construction and different coating of the laser mirrors. The experimental results obtained by thermoreflectance (TR) mapping are compared with calculated temperature distributions. To verify the calculated data, we have developed a new technique to monitor the laser facets heating in real time and to correlate these measurements with device performance and reliability. The method is based on TR, which is a modulation technique relaying on periodic facet temperature modulation induced by pulsed current supply of

the laser [1]. The periodic temperature change of the laser induces variation of the refractive index and consequently modulates probe beam reflectivity. TR technique provides information about real mirror temperature distribution and the absolute value of the temperature is proportional to the signal intensity. The scaling factor is different for different types of lasers and depends on composition and doping of the active region and type of mirror coating. In this work we have used micro-Raman spectroscopy to determine the scaling factor for each particular LD [2, 3]. Raman spectroscopy is not sensitive to coating type and gives direct information about absolute temperature. Combining the TR and micro-Raman techniques allows us to achieve real temperature maps of the LD mirrors.

As an additional technique we have used imaging thermography in the 3–5 μm wavelength range [4–6]. This technique, however, is not directly connected to the mirror surface temperature. Due to the fact that all semiconductor layers of LD are transparent for the above wavelengths, the image produced by the thermographic camera is rather connected to the temperature inside the LD and not the temperature at the mirror surface. Nevertheless, the imaging thermography in conjunction with the other techniques provides useful information about thermal problems related to the device operation. In particular it allows to estimate the difference between the temperature in the bulk and at the surface of the mirror, which is an important indication of the mirror degradation processes.

2. Samples and experiment

The broad-area devices are based on double-barrier separate confinement heterostructures designed for 808 nm emission wavelength. The 15 nm thick tensile strained GaAsP active quantum well is surrounded by 140 nm (sample A) and 130 nm (sample B) thick $Al_{0.3}Ga_{0.7}As$ barrier layers, followed by 150 nm (sample A) and 30 nm (sample B) thick $Al_{0.7}Ga_{0.3}As$ outer anti-waveguide layers, which are graded toward the $Al_{0.45}Ga_{0.55}As$ claddings. Thickness of graded layers and cladding layers in both samples was equal to 30 nm and 3 μm, respectively. The emitting stripes of about 100 μm width are formed by H^+ implantation. The laser facets are asymmetrically coated with AlN-Si/AlN multilayers. Devices were In-soldered, *p*-side down onto copper heatsinks. Typical threshold current densities were of the order of 250 Acm^{-2} for the devices having a cavity length of 1 mm. Figure 1 shows calculated band lineup versus growth direction for both types of the structures investigated calculated with the Nextnano software.

The TR relies on periodic facet temperature modulation induced by pulsed current supply of the LD. The device is mounted on the high precision *x*-*y*-*z* piezo-stage to align the laser mirror against the probe laser beam which is reflected from the facet. The probe beam spot size is diffraction limited and can be as low as 0.6 μm for the probing beam wavelength λ = 422 nm. The spatial resolution is determined by the probe beam spot size. The beam spot and the laser facet are observed with CCD video camera

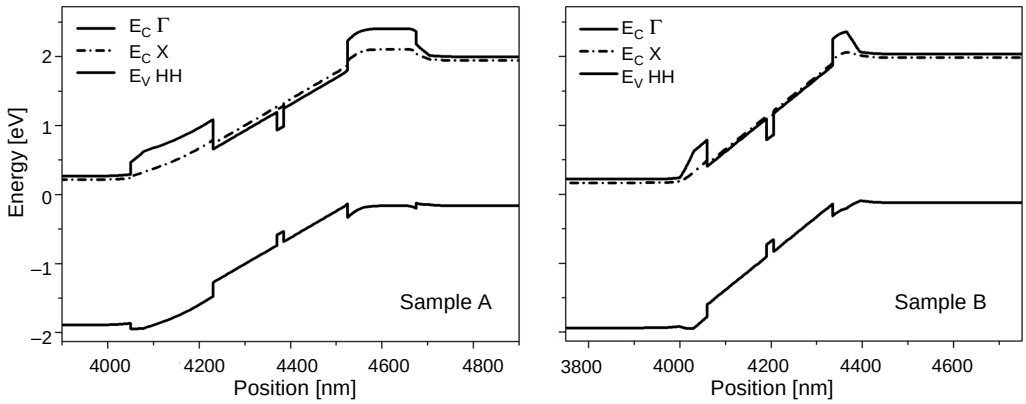

Fig. 1. Band lineup in the samples *A* and *B* with no polarization applied.

and monitor under high magnification, which allows for accurate probing of specific regions of the laser. The use of piezoelectrically driven translator stages allows for obtaining maps of the temperature distribution over the laser facet. The laser is supplied with low frequency pulsed current (50–200 Hz) with filling factor 50%. Under these conditions the laser is operating in the quasi-CW mode and is subjected to the thermal effects associated with CW operation. The periodic temperature change of the laser induces variations of the refractive index and consequently modulates probe beam reflectivity. A probe beam coming from a He-Cd laser (λ = 442 nm) enters a commercial microscope and is focused on the sample surface. The typical probe beam power on the sample's surface is about 100 μW. The beam is reflected back by the surface of the sample and directed on the Si photodiode by a beam splitter. The output signal from the Si detector is analyzed with a lock-in amplifier, and its DC component is used to normalize the signal, giving the experimental values of relative reflectance changes. The back side of the laser submount is temperature controlled by Peltier cell.

The absolute facet temperature measurements were carried out with a conventional micro-Raman setup based on 0.6 m Dilor spectrometer equipped with a liquid-nitrogen -cooled CCD-multichannel-detector. The 514.5 nm emission of an Ar^+ ion laser served as the CW excitation source. The laser beam was focused onto a test device by using a microscope. A spot diameter of ~1 μm, determined by using knife-edge method at the LD heterointerface, has been achieved. The back-scattered light from the sample was collected through the same microscope, then fed into the triple path spectrometer. The increase in the biased LD mirror temperature has been determined from the wavelength shift of the Stokes–Raman line. TR and micro-Raman techniques use similar probe beams and focusing system, therefore temperature determined from the micro-Raman measurements can be used for scaling TR maps.

The imaging thermography has been performed with the THERMOSENSORIK CMT 384M camera, equipped with 384×288 pixel HgCdTe detector. It operates in 3–5.5 μm wavelength range with the nominal spatial resolution of about 5 μm.

3. Results

Spatially resolved TR maps were measured for laser samples *A* and *B* operated above threshold at different supply currents. Due to the differences in coating layer thickness between particular LDs, the intensity of TR signal was different for samples *A* and *B*. To achieve strong TR signal for sample *A*, operation current was 400 mA. In the case of sample *B* we had to apply higher current (800 mA) to attain signal strong enough to make a clear map. Figure 2 presents temperature distribution maps for samples *A* and *B* operated under 400 and 800 mA, respectively. The cross-sections of the TR maps along the lines parallel to the epitaxial layers are shown together with the maps of relative temperature distribution.

In TR maps we can evidently distinguish darker stripe at the bottom. This stripe corresponds to the epitaxial layers, whereas the rest of the map corresponds to the substrate. In the case of the experimental set-up used the energy of the probe beam is 2.8 eV, which is close to the energy of the GaAs E_1 critical point. Due to that, the signal related to GaAs is much stronger than the signal related to the ternary AlGaAs with high Al concentration, which is a predominant constituent of the epitaxial layer structure of the laser. To recalculate TR maps into temperature maps, we have to use scaling factor and for the structures investigated scaling factors for GaAs substrate and for the epitaxial layers are essentially different. We can expect that for the hottest area in the middle of epitaxial layer, where the TR signal is of relatively lower intensity, the scaling factor is much higher than for GaAs substrate. After performing a micro-Raman calibration of thermoreflecance, as it is described below, we have

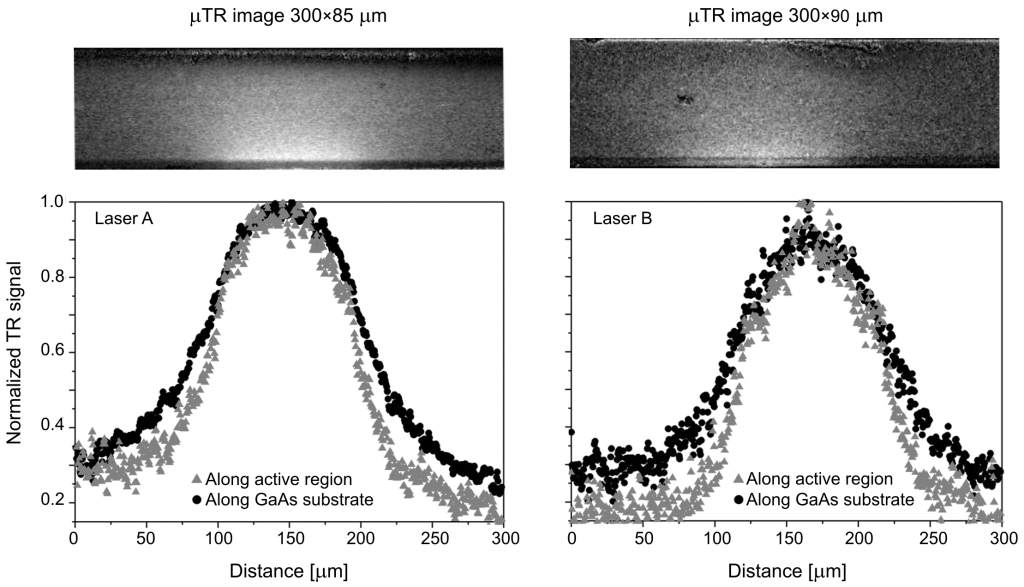

Fig. 2. TR maps of laser samples *A* and *B* operated at 400 and 800 mA, respectively. Also shown are line scans of temperature distribution in the epitaxial active region and GaAs substrate.

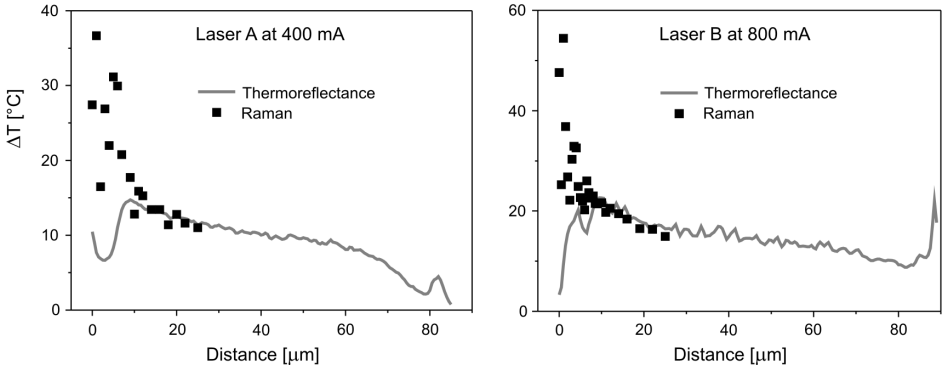

Fig. 3. Temperature of the laser mirrors determined by TR and micro-Raman measurements. The respective curves show temperature in the middle of the mirror along the axis perpendicular to the epitaxial layers.

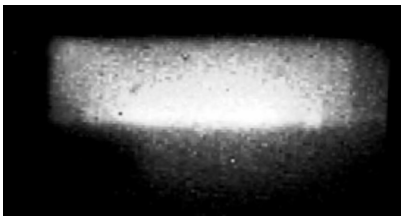

Fig. 4. Thermographic image of the front facet of the LD operated at 800 mA.

found that response of GaAs for the probe beam wavelength is roughly twice stronger than the response of epitaxial layers.

The measured temperature distributions at the front facet of semiconductor LD are shown in Fig. 3. The curves shown in Fig. 3 were obtained from vertical line scans starting at the edge of the *p*-type contact and going towards the substrate. Solid lines represent results obtained by TR method; points represent results obtained by micro-Raman spectroscopy. The apparent temperature drop in the region of epitaxial layers, as evidenced by TR, is the result of using the calibration factor for the recalculation of the relative reflectance changes into temperature, which is appropriate for GaAs substrate but not for the laser structure as a whole. This approach is evidently not correct for epitaxial layers part of the structure. The temperatures derived from TR and micro-Raman spectroscopy can be matched-up by using two different calibration factors for epitaxial layers and GaAs substrate to recalculate experimental data.

The micro-Raman measurements are not sensitive to surface passivation, coating thickness and quality. The combination of the two techniques, *i.e.* micro-Raman and spatially resolved TR, gave us true information about the absolute value of mirror temperature and its spatial distribution. For each particular examined LD type it is, however, necessary to find a proper TR scaling factor using micro-Raman measurements.

The fastest method of monitoring the LD temperature is capturing infrared radiation emitted by the device using thermographic camera.

With thermocamera we can monitor LD temperature in real time. Figure 4 presents thermocamera image of LD operated at supply curret equal to 800 mA. Presented image relates to the bulk temperature as it has been stressed earlier. Observed temperature distribution is averaged along Fabry–Perot resonator because LD is transparent in thermographic camera spectral region of operation. Nevertheless, the thermocamera image is an interesting supplement of the surface related data.

4. Conclusions

Using spatially resolved thermoreflectance and micro-Raman technique, we have been able to achieved complete picture of the laser diode front facet temperature distribution. The possibility of experimental determination of temperature distribution on a microscale on operating devices is a milestone in determination of the heat sources in LDs and contributes significantly to the understanding of facet degradation mechanisms. It can also help to resolve design issues related to thermal management in LDs, as well as to optimize mounting and heat-sinking problems. These are the major factors that influence device reliability. The experimental data are accurate enough to be directly compared with calculated 2D temperature profiles, which provides an additional factor in the laser optimization process. So far there were no experimental methods which could provide temperature distribution maps on working devices with such high spatial resolution which is required for examination of complex semiconductor laser structures.

Acknowledgements – This work was partially supported by Polish Committee for Scientific Research Grant No. 3T11B03128.

References

[1] EPPERLEIN P.W., BONA G.L., ROENTGEN P., *Local mirror temperatures of red-emitting (Al)GaInP quantum-well laser diodes by Raman scattering and reflectance modulation measurements*, Applied Physics Letters **60**(6), 1992, pp. 680–2.

[2] TODOROKI S., SAWAI M., AIKI K., *Temperature distribution along the striped active region in high-power GaAlAs visible lasers*, Journal of Applied Physics **58**(3), 1985, pp. 1124–8.

[3] BRUGGER H., EPPERLEIN P.W., *Mapping of local temperatures on mirrors of GaAs/AlGaAs laser diodes*, Applied Physics Letters **56**(11), 1990, pp. 1049–51.

[4] SHVYDKA D., RAKOTONIAINA J.P., BREITENSTEIN O., *Lock-in thermography and nonuniformity modeling of thin-film CdTe solar cells*, Applied Physics Letters **84**(5), 2004, pp. 729–31.

[5] ALBRIGHT G.C., STUMP J.A., MCDONALD J.D., KAPLAN H., *True temperature measurements on microscopic semiconductor targets*, Proceedings of the SPIE **3700**, 1999, pp. 245–50.

[6] ALBRIGHT G.C., STUMP J.A., LI C.P., KAPLAN H., *Emissivity-corrected infrared thermal pulse measurement on microscopic semiconductor targets*, Proceedings of the SPIE **4360**, 2001, pp. 103–11.

Received June 6, 2005
in revised form November 3, 2005